



How to Estimate the Major Petrophysical Properties: A Review

Rusul A. Hashim¹ and Ghanim M. Farman^{1,*}

¹Department of Petroleum Engineering, College of Engineering, University of Baghdad.

Article information

Article history:

Received: February, 23, 2023

Accepted: March, 30, 2023

Available online: April, 08, 2023

Keywords:

Petrophysical Properties,
Hydrocarbon, Reservoir,
Shale Volume,
Porosity,
Water Saturation,
Permeability

*Corresponding Author:

Ghanim M. Farman

ghanimzubaidy@uobaghdad.edu.iq

Abstract

Petrophysical property estimation is critical for reservoir predictions. It generally encompasses all coring, logging, testing, and sampling procedures. Almost 50 years ago, the evaluation of subsurface formations related to drilling oil wells got involved. It involves all techniques for coring, logging, testing, and sampling in general. It focuses on the process of interpreting logs and how to conduct lab tests that are important for evaluating formations below the surface, including a look at the fluids they represent. The casing is occasionally set to analyze the formations with more accuracy; as a result, this process is also considered. The scientific field of petrophysics of reservoir rocks is interested in researching porous materials' physical and chemical characteristics and the elements of reservoir rocks connected to pore and fluid distribution. Much research on the characteristics of various rocks, including their porosity, permeability, capillary pressure, hydrocarbon saturation, fluid properties, electrical resistivity, self- or natural potential, and radioactivity, has been carried out in recent years. The existence or absence of economic quantities of hydrocarbons in formations penetrated by or around the wellbore is assessed using these qualities and their relationships. This paper's main goal is to evaluate the historical evolution of the most popular methods for calculating petrophysics parameters in the lab and on the ground, mostly based on the researchers' scientists' knowledge of that field.

1. Introduction

Interpreting well-log r is critical for engineers and geologists to categorize petrophysical parameters. The log data is critical in reservoir engineering calculations, particularly in estimating reserves. The optimum interpretation for any structure of interest is impacted by the quality and quantity of log data accessible to analysts, as well as the type of Problem [1]. When examining these qualities, there are two forms of data to consider: Instrumental techniques that measure the attributes vs. depth, known as logs, and actual samples that accurately replicate the formation under consideration, such as cores and cuttings [2]. Cross-plot techniques are often used to demonstrate the influence of log combinations on lithology and porosity, and they provide a visual representation of the kind of lithology mixes [3].

The quantitative assessment of a hydrocarbon unit in any formation needs an accurate estimate of shale volume, which blocks the pore space and reduces the amount of permeability, lowering reservoir quality [4].

Porosity can be calculated in various ways, including laboratory testing and log data. The accuracy of porosity determined from drill cuttings can be greatly influenced by cutting size and desaturation time [5].

Similarly, log analysis has been used to determine porosity. Water saturation (S_w) is an important aspect of formation evaluation that is currently challenging to assess via well-logging analysis. The Archie formula was initially established for clean development to estimate water saturation based on resistivity and porosity. Following that, a slew of major water saturation models for shale-bearing sands arose, including the Simandoux model and the modified Simandoux model [6]. Indonesian model, total shale model, modified total shale model, dispersed clay

model, and dual water model. That leads to good results for clean sandstone reservoirs.

For petroleum engineers, permeability is a main input and key in reservoir management and development. For example, when selecting the optimum production rate for the field and water injection patterns [7]. These properties and their correlations determine the existence or absence of economic amounts of hydrocarbons in formations penetrated by the wellbore or lying near. The primary objective of this study is to evaluate the evolution of the most prevalent approaches used to determine petrophysics parameters in the laboratory and field, based mainly on researchers' and scientists' own experience in this field.

2. Materials and Methods

The petrophysical parameters were subjected to a range of parameter approaches. The subdivisions that follow provide a quick overview of various approaches.

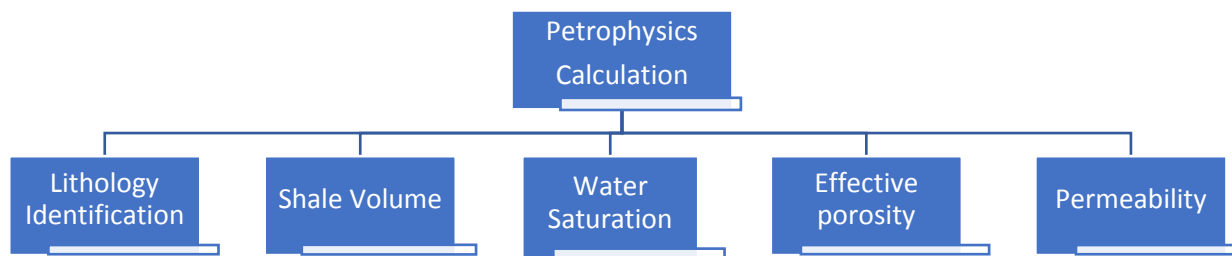


Figure 1: Petrophysical Analysis and Flow Units Characterization.

2.1 Shale volume Estimation Methods

Estimating the volume of shale in the formation is the first step in the reservoir characterization, formation evaluation, and log interpretation processes because it is necessary to determine the formation's porosity and fluid content [11][12]. The presence of shale in the formation has a variety of effects on the response of logging tools (Adeoti et al., 2009)[10] and the petrophysical characteristics of the reservoir, reducing its effective porosity and permeability and increasing the uncertainty surrounding the evaluation of the formation and reservoir characterization [11]. This section will deal especially with how shale volume determination in the formation is determined by logging devices such as gamma ray, neutron density log, resistivity log, and sonic log. The oldest study on the connection between resistivity and the saturation concept indicates [8].

Poupon and Leveaux (1971) used a computer-generated a cross plot equation between the water saturation (Sw) and true resistivity of the formation, the range of shale recorded (30-70%) [12]. An Indonesian model was developed to calculate high amounts of shale and freshwater saturation.

$$\frac{1}{\sqrt{Rt}} = \left[\frac{V_{cl}}{\sqrt{R_{clay}}} + \frac{\phi^{\frac{m}{2}}}{\sqrt{a \cdot R_w}} \right] * S_w^{\frac{n}{2}} \quad (1)$$

where V_{clay} is volume of shale; Rt, formation true resistivity; R_w, formation water resistivity; a, tortuosity; φ, porosity; S_w, water saturation.

Clavier (1971) developed an equation that was used to estimate shale volume using gamma ray, density, and neutron-density approaches [13],[14]. Total and effective porosities for older rocks were computed using total and effective porosities. Clavier neutron-density equation [16]:

$$V_{sh} = \frac{NPHI_{log} - NPHI_{ma} + M_1(\rho_{ma} - \rho_{log})}{NPHI_{shale} - NPHI_{ma} + M_1(\rho_{ma} - \rho_{shale})} \quad (2)$$

The gamma-ray index must be determined using the following formula to determine how much shale is present.

$$IGR = (GR_{log} - GR_{min}) / (GR_{max} - GR_{min}) \quad (3)$$

Then, according to Serra (1984), one may use the following calculation to get the shale volume (V_{sh}) using the Gamma-ray index [15]:

$$V_{sh} = 0.33[2(2 \times IGR) - 1.0] \quad \text{for hard formation} \quad (4)$$

$$V_{sh} = 0.083[2(3.7 \times IGR) - 1.0] \quad \text{for soft formation} \quad (5)$$

$$V_{sh} = IGR / [3 - 2IGR] \quad \text{for gas-saturated formation} \quad [4] \quad (6)$$

Hughes (1992), the resistivity device used as a clay indicator is based only on the differential between the resistivity response in shale and a clean pay zone. The basic equation is [18]:

$$V_{clay} = \left(\frac{R_{cl}}{R_t} * \frac{R_{lim} - R_t}{R_{lim} - R_{cl}} \right)^{(1/1.5)} \quad (7)$$

Where R_c : Resistivity of clay (Adjacent Shale Bed), R_t : Resistivity of shaly sand, R_{lim} : Resistivity of a clean hydrocarbon zone.

Also, Hughes (1992) measured shale volume from the neutron record, which is the content of the formation of hydrogen by sending neutrons to the formation, and this content of hydrogen can be determined. The following neutron equation for determining the volume of clay is shown[18]:

$$V_{clay} = \frac{\phi_{Nlog}}{\phi_{Nclay}} * \frac{\phi_{Nlog} - \phi_{Nmim}}{\phi_{Nclay} - \phi_{Nmim}} \quad (8)$$

Bassiouni, in 1994 estimated the shale volume from a sonic log, and this method calculates the acoustic logarithm of the shale volume in the formation. The acoustic equation for estimating clay volume is given below [17]:

$$V_{clay} = \frac{\phi_s(\text{shaly sand})}{\phi_s(\text{shale zone})} \quad (9)$$

Where φ_s (Shaly Sand): Sonic porosity at the shaly sand interval, φ_s (Shale): Sonic porosity at the shale interval. While Adeoi, Ayolabi, E.A., and James (2009), the shale volume was calculated by adopting neutron porosity and density. This method relies on the neutron response and density in oil shale to calculate the clay volume. The characteristics of the clean matrix (neutron values and sand density values) must be recognized or neglected. When clay content increase, so does the difference between neutron porosity and density. The equation represents the calculation of clay volume using neutron density [10].

$$V_{clAY} = \frac{\phi_N(\text{shaly sand}) - \phi_D(\text{shaly sand})}{\phi_N(\text{shale zone}) - \phi_D(\text{shaly zone})} \quad (10)$$

Where V_c : Clay volume, φ_D (Shaly Sand): Density porosity at shaly sand zone; φ_N (Shaly Sand):

Neutron porosity at shaly sand zone; ϕN (Shale): Neutron porosity at shale zone; ϕD (Shale): Density porosity at Shale zone. The shale volume was also measured using the sonic-density method. The following is the sonic-density

The equation for determining clay volume [10]:

$$V_{clay} = \frac{\phi_s(\text{shale sand}) - \phi D(\text{shale sand})}{\phi_s(\text{shale zone}) - \phi D(\text{shale zone})} \quad (11)$$

Finally, they used the neutron-sonic method, which is rarely used to calculate the mud content in shale sand formations because both neutron and sonic tools are strongly affected by mud. The neutron sonic equation for slurry volume calculation is given below [10]:

$$V_{clay} = \frac{\phi N(\text{shale sand}) - \phi_s(\text{shale sand})}{\phi N(\text{shale zone}) - \phi_s(\text{shale zone})} \quad (12)$$

This means there are two groups for measuring the shale volume, where the first group measured it. The single clay index method contains a segmented method used to calculate the clay volume (gamma ray log, sonic log, deep resistivity log, and neutron log). While there are three types of dual indices: the volume of clay from logs measured in terms of neutron density, neutron sonic, and clay volume (acoustic density). Mud volume results are either too low or too high when utilizing the neutron density technique to estimate mud volume due to well conditions. Due to the possibility that the distributed mud might affect the sound waves, mud oil from the Density and Sonic recordings cannot be accounted for in all shales. Water Saturation Estimation Methods

2.2 Water Saturation Estimation Methods based on the resistivity log

Water saturation based on resistance is considered the most reliable method and is more accurate when used in the Virgen zone. The determination of saturation in the Clen formations will be covered separately in this section; Resistivity is recorded by logging devices like later log or induction as just an apparent value (qualitative measurement), which is influenced by several factors like drilling fluid type or invasion. Archie (1942) offers an experimental method for extending and enhancing the electrical well-logging interpretation technique for clean and homogenous formations (limestone) saturated with water. This is the earliest investigation of the link between resistivity and saturation concept. The main goal of Archie's study was to present some of these laboratory data and to suggest their application to quantitative studies of the electrical log. It should be noted that various experimental research investigations of the formation of physical features in connection with electrical observations have been conducted. To determine oil or gas saturation by electrical log, he analyzed the formation resistivity when all pores are filled with water as indicated in the correlation below [19]:

$$R_o = F \times R_w \quad (13)$$

Where R : Formation resistance when the water is completely saturated. R_w : Water formation resistivity, and F : formation resistivity factor. F is a function of type and characteristic of formation and varies based on porosity (ϕ), and Permeability(K), from the laboratory, the measurement of the more variable effect on F is the porosity, so the Empirical form of the equation is:

$$F = 1/(\phi^m) \quad (14)$$

The cementing factor or porosity exponent (m) is one of the most important Archi parameters, a major source of uncertainty in calculating water saturation for a carbonate reservoir. The parameter m is not a constant, particularly in heterogeneous reservoirs; its value depends on the type and percentage of the porosity. When applying Archie's Equation [19], an inaccurate assessment of m might result in substantial mistakes in the water saturation computation. Such cementation factor uncertainty always has a large impact on the hydrocarbon saturation values [20]. The Archie porosity exponent, " m ," or cementation factor, is crucial in determining the early water and oil saturations. The Archie equation describes the relationship between porosity, water saturation, and formation water resistivity. It is formulated as follows:

$$S_w^n = (a R_w) / (\phi^m R_t) \tag{15}$$

$$S_{xo}^n = ((a R_{mf}) / (\phi^m R_t)) \tag{16}$$

Where: n: is the saturation exponent, (Empirical solution 1.2-2.2), S_{xo} : water saturation of flashed zone, R_{mf} : Mud filtrate resistivity and R_{xo} : shallow formation resistivity. Companies develop resistivity scales based on the electrode being a point in a homogenous bed. Archie considers the variables that may influence resistivity results, such as the presence of a borehole, thickness, and invasion, to be rectified. The following authors also describe this approach for estimating water saturation properties in clean formations.

2.2.1. Water Saturation from the resistivity concept in clean formation

(Tixier, 1958) provides an example of the phrase "porosity balancing," which describes a confirmation of saturation values obtained from logs using one of the resistivity ratio methods: The first three methods are the Induction-Electrical Log, Rocky Mountain, and R_{xo}/R_t . The porosity balancing check entails calculating a value for the formation factor (F) using the saturation value obtained using one of the aforementioned techniques and contrasting this computed formation factor with the formation factor (or, equivalently, the porosity) acquired from other independent sources. Generally speaking, if the computed formation factor is too low, the corresponding saturation value is too low; conversely, if the calculated formation factor is too high, the corresponding saturation value is too high [21].

2.2.1.1 Induction-Electrical Log Method

The Induction-Electrical log interpretation chart (Schlumberger, n.d.) was used to discover the approximation of water saturation, and Archie's equation with the new form, as shown below, was used to compute the formation factor (F) was then compared with an independent technique to confirm the accurate value of SW [22].

$$F = \frac{R_t}{R_w} \times S_w^2 \tag{17}$$

R_w has previously been estimated with S_p or the direct analysis approach, and R_t is calculated with the induction resistivity log.

2.2.1.2 Rocky Mountain Method

The relations offer the oldest resistivity ratio technique's water saturation and formation factor.

$$S_w = \frac{R_i}{R_t} * \frac{R_w}{R_z} \tag{18}$$

$$F = R_i^2/R_t \times R_w/R_z^2 \tag{19}$$

Where R_i is the short normal resistivity, and R_z is the resistivity of mixed connate and filtrate water, compare F computed and F's genuine value.

* When F calculated using Eq. 9 is less than the real value of F: This shows that the water saturation calculated using Eq. 8 is too low.

* When F calculated using Eq. 19 exceeds the correct value of F, it shows that the water saturation calculated using Eq. 8 is too high.

Since water saturation and formation factor are very sensitive to resistivity value, it is advised to employ this approach in medium and hard formations when $R_{16}/R_m > 10$ and neither nighttime micro-log nor microliters-log are available.

2.2.1.3 R_{xo} , R_t Method

R_{xo} may be calculated precisely using the Micro-log or Microlatero-log, and R_t using deep investigation equipment used in the case of salty muds and hard formations. As a result, the approximation of this technique is shown below.

$$S_w = \left[\frac{R_{xo}}{R_t} \times \frac{R_w}{R_{mf}} \right] \quad (20)$$

based on assumption $S_{xo} = S_w^{1/5}$ (21)

$$F = \left[\frac{R_w}{R_{mf}} \right]^{5/4} \left[\frac{R_{xo}^5}{R_t} \right]^{1/4} \frac{1}{R_w} \quad (22)$$

When F is less than the right value of (F), it shows that $(R_{xo}^5/R_t)^{1/4}$ is too low, and SW is low. In contrast, if F is bigger than the true F, Sw is too large, as computed by the technique.

(Pickett, 1966)[23] and (Pickett, 1973)[24] have developed some techniques to calculate water saturation, such as,

2.2.1.4 Apparent Resistivity vs. Apparent Porosity Plots

The method presents a graphical solution to Archie's equation for determining reservoir water saturation by graphing resistivity vs. porosity on a log-log scale. The following are the advantages of this method: (1) A large amount (fluid) of the section can be quickly assessed in wells with little petrophysical data. (2) No prior knowledge of water resistivity or the cementation factor is required. The graph paper-driven general equation convention is as follows [25]:

$$\log(\emptyset) = \log(a \times R_w) - \frac{1}{m} \log(R_t) - n \log(S_w) \quad (23)$$

A Pickett plot with a mixture of water and hydrocarbon zone points yields the following features [26]:

- 3 Different porosity water-bearing ($S_w = 100\%$) points are plotted along a straight line with a slope of $(-1/m)$ and an intercept of $(\text{an } R_w \text{ @ Porosity}=100\%)$. In contrast, the cementation exponent (m) and R_w may be predicted if the tortuosity factor (a) is known (or assumed).
- 4 Hydrocarbon-bearing (S_w less than 100%) sites are positioned at a distance. Their higher resistivity causes them to move horizontally to the right of the water-bearing line, dependent on water saturation distribution. If the saturation exponent (n) is known, the water saturation may be determined (or can be assumed). Lines of constant water saturation run parallel to the water-bearing line. Although porosity is now frequently depicted on the Pickett plot, Pickett utilized two extra parameters ($\rho_b - \rho_{ma}$) instead of density porosity [27] and $(\Delta t - \Delta t_{ma})$ instead of sonic porosity [28].

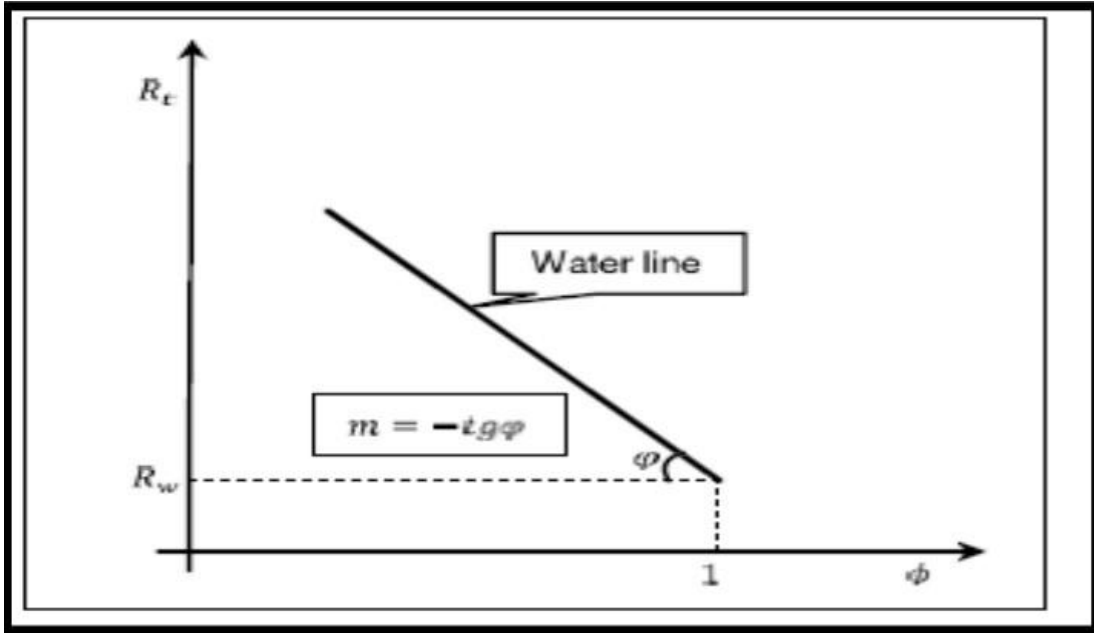


Figure 2: Pickett plot[24].

2.2.1.5 R_{wa} Vs. Depth plots

$$R_{wa} = R_t / \phi^m \tag{24}$$

When the water resistivity is unknown, these assessment procedures come in handy. If the ratio of the R_{wa} for any interval is 4 or larger when compared to the minimum R_{wa} , the interval most likely has a water saturation of less than 50%. If the ratio is between one and four, the method shows that the interval most likely includes some hydrocarbons. The approach has the disadvantage of requiring continual water resistance.

2.2.1.5 Hingle plot

A graphical solution was proposed. It was the first answer to Archie's equation that was widely adopted. Use a specially prepared graph paper to understand this approach and search for the cementation exponent value, m , where the y-axis fluctuates with that value. Assume that the saturation exponent and cementation exponent are both equal to 2.0 and rewrite the Archi formula as follows [29]:

$$\frac{1}{\sqrt{R_t}} = S_w \frac{1}{\sqrt{R_w}} \phi \tag{25}$$

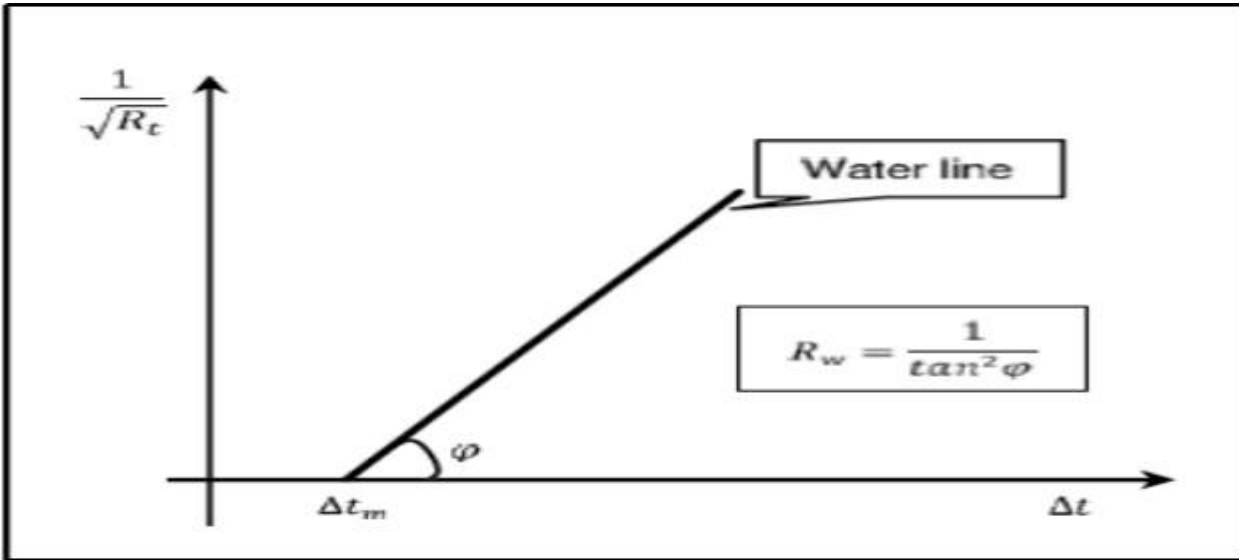


Figure 3: Hingle plot [29].

2.2.2. Water saturation from the resistivity concept in shaly formation.

(Leveaux and Poupon, 1971; Poupon et al., 1954) in the laminated shaly sand model by constructing an empirical connection utilizing computer cross-plots that produced noticeably better outcomes in several Indonesian wells as shown below[30][31]:

$$S_w = \sqrt{\left(\frac{a R_w (1-V_{sh})}{\phi^m} + \left(\frac{R_{sh}-V_{lam}.R_t}{R_{sh} R_t}\right)\right)} \tag{26}$$

Where:

Rsh: is the mean value of the shale's deepest resistivity curve measurement (Ohm.m).

Vsh: Denotes the volume of shale in the formation (%).

Vlam: is the percentage of laminated shale volume in the formation (%), and

φ: denotes the overall porosity (%).

(Simandoux, 1963) created a model for predicting water saturation during the production of shale sand. In response to laboratory experiments conducted on a physical product, the model was developed. In the Institute of English Petroleum, a reservoir model built of synthetic sand and clay, was constructed (IFP). Simandou still exists. One of the most popular models for water saturation models and a crucial foundation for further study in this area. The Simandoux formula [32]:

$$S_w = \frac{a \cdot R_w}{2 \cdot \phi^m} \left[\left(\frac{-V_{sh}}{R_{sh}}\right) + \sqrt{\left(\frac{V_{sh}}{R_{sh}}\right)^2 - \left(\frac{4\phi^m}{a R_w R_t}\right)^2} \right] \tag{27}$$

Poupan and Leveaux (1971) developed a technique for calculating water saturation in stratified shales. The Indonesian equation is a common term for this concept since it was built using field findings from Indonesia. As illustrated below[30][31]:

$$S_w = \frac{1}{R_t} \left[\frac{\sqrt{a R_w R_{sh}}}{V_{sh} \sqrt{a R_w} + \phi^m \sqrt{R_{sh}}} \right]^{n/2} \tag{28}$$

This type of relationship between Rt and Sw expresses that the formation's conductivity is made up of three components, the first two of which are the conductivities of the clay and formation-water networks, and the third is the additional conductivity caused by the cross-linking of these two networks.

(Waxman and Thomas,1974)[33] Hence, the Waxman-Smiths equation is empirically confirmed for analyzing resistivity logs in hydrocarbon-bearing shaly sands. The water-bearing equation has been used successfully

to describe shale conduction [34].

$$S_w^{-2} = \left[\left(\frac{R_t}{R_w} \right) * \phi^m \left(1 + \frac{R_w B Q_v}{S_w} \right) \right] \quad (29)$$

where B is the temperature-dependent equivalent cationic conductance of a sodium ion, and Q_v is the cation exchange capacity per unit pore volume, which varies depending on the type of clay. m and n are similar to Archie but are derived from core data differently. The effective concentration of clay-exchange cations increases in proportion to the decrease in water saturation, based on the results of the experiments.

Clavier and colleagues (1984) According to the Dual-Water concept, clay-bound and non-clay water act as two parallel conductive layers contributing to overall conductivity (C_t). The Dual-Water model looks like this [15]:

$$C_t = \phi t^{-m} \times S_w^n \left[C_w + \frac{V_Q Q_v (C_{cbw} - C_w)}{S_w} \right] \quad (30)$$

C_{cbw} : conductivity of clay-bound water, S_m^{-1} ;

Q : cation exchange capacity per unit pore volume, meq cm^{-3}

V_Q : the amount of clay water associated with milliequivalents of clay counterions, meq- $1cm^3$;

The Archie variables can be used to estimate the parameters (m, n).

The dual model can also represent a function of resistivity as follows [58]:

$$\frac{1}{R_t} = \frac{S_w^2}{F R_w} + \frac{B Q_v \times S_w}{F} \quad (31)$$

2.3 Porosity Determination methods

There are several forms of porosity, defined as the proportion of the pore or void volume to the macroscopic or bulk volume. The bulk Darcy flux is related to the average flow in pores. It ranges from 0.1 to 50%.

2.3.1 Porosity measured in the laboratory by (collecting cutting):

(Onyia, 1988) Warren's roller cone penetration rate model describes the relationship between UCS and porosity. In this case, the log and drilling data are used to estimate the UCS directly. Shale and sandstone are two lithologies that the Onyia approach applied to [35].

To evaluate the porosity, Vojko Matko 2003 used the stochastics method, which uses a highly sensitive sensor with minimal measurement errors and interference from noise signals. Compared to using helium pycnometers, it is much easier. In addition, the material is not wetted. Instead, water is used to submerge the soil or rock sample. The porosity sensor uses capacitive-based sensitive crystals with a frequency of 40MHz and temperature stability of 1ppm for long-term repeatability and stability. The direct digital method (DDM) minimizes the influence of perturbation, thus reducing the uncertainty of the outcome [36].

(Erfourth et al., 2006) This method calculates porosity using UCS data gathered through laboratory examination of core, cast, and tuff samples. The Erfourth approach becomes inaccurate for high UCS sectors, whereas the Onyia

method produces significantly greater porosity values for low UCS sectors than the Erfourth method. At a UCS value of 100 MPa, the Onyia correlation stabilizes [37].

(Abassi et al., 2013) In this study, the researchers measured the longitudinal ultrasound velocity, porosity, and tortuosity of meteorites using an ultrasonic reflectivity approach. At two oblique angles of incidence and normal incidence, the ultrasonic reflection coefficient of polished meteorite thin plates was determined. This approach is easy, quick, cheap, and non-destructive compared to other existing laboratory processes for evaluating porosity. They found a strong linear relationship between density and porosity in the meteorite specimens they had studied, as well as a strong linear relationship between the logarithm of porosity and the longitudinal velocity of ultrasound. This shows that a straightforward linear mathematical formula based on the longitudinal velocity of ultrasonic vibrations may be used to determine the porosity of these meteorites[39].

2.3.2 Porosity measured in the laboratory from Drilling Data:

Westbrook and Redmond, in 1946, applied a single-unit arrangement study of the capillary diaphragm. This

method offered a way to calculate the bulk volume of many particles, including drill cuttings. This technique is highly precise and avoids inaccuracies shown in previous methods of determining the porosity of drill cuttings [38].

Chang and Horsund, in 2001, The Gamma Rays technique was employed by the researchers in this study to gather information from both the core and cuttings analyses. To establish real relationships between the UCS and porosity in sandstone and shale lithologies, as well as between these two variables [39].

(Siddiqui et al., 2005) This study used laboratory equipment to crush the plug into cuttings with different mesh sizes to display the full description of a carbonate core plug. The cutting samples were then scanned using a C.T.-scanner to measure the (bulk densities and porosities) [40].

Fonta and Lenormand, in this study, reconsideration of the CT-scan technology, which is used in the medical field, and showed that accuracy was worse for cuts with a diameter of less than 2.5 mm. Cutting with diameters as small as 0.5 mm will provide consistent porosity [41].

2.3.3 Porosity measured from Well log

When the matrix lithology is unknown or comprises two or more unknown characteristics minerals, determining the accurate porosity is complex. Single-log and double-log indicators can be used to determine porosity. The single log method for calculating porosity uses measurements of density, sonic, and neutrons. In contrast, the double log method for calculating effective porosity uses a combination of neutron-density logs and neutron-sonic logs. According to Hamada (1996), the Neutron-Density equation [42]:

$$\emptyset_e = \frac{\emptyset_N + \emptyset_D}{2} \quad (32)$$

Where \emptyset_e : Effective porosity from Neutron-Density logs; \emptyset_N : Porosity by Neutron log; \emptyset_D : Porosity by Density Log.

The porosity can be calculated by neutron-sonic equation [42]:

$$\emptyset_e = \frac{\emptyset_N + \emptyset_S}{2} \quad (33)$$

(Taud et al.,2005) It is frequently stated as a proportion of space relative to an object's overall volume [43]:

$$\text{Porosity}[\%] = \frac{(\text{Volume of pores})}{(\text{Volume of solid (incl.pores)})} \times 100 \quad (34)$$

2.4 Permeability Determination methods

Typically, permeability statistics are collected by regular analysis in the field or laboratory. Core analysis is one of the most accurate methods for determining permeability, although expensive and time-consuming. Well-testing can provide an average permeability value and information on the reservoir's extent and connection. More precise permeability data may be obtained using the (MDT) approach. The NMR log is now routinely utilized to provide a quick estimate of the permeability profile along the wells. The essential methods for measuring permeability have been developed:

Carman-Kozeny developed a formula to assess permeability (k). This computation produced a mixture of Poiseuille's and Darcy's laws. Poiseuille's law describes the parabolic displacement of a viscous fluid in a straight-circular tube, whereas Darcy's law quantifies fluid flow macroscopically. The semi-analytical Carman-Kozeny (C.K.) equation fails to adequately represent the relationship between permeability and porosity because (a) it was developed for a solid medium with pipe conduits rather than a granular medium, and (b) even if a grain size is included in the equation, it is not immediately clear that it does not change as porosity changes [44][45].

$$Dh = \frac{4 \varepsilon V}{Sv} + \frac{4 \varepsilon}{(1-\varepsilon)av} = \frac{\varepsilon d}{(1-\varepsilon)} \quad (35)$$

$$\text{Where } av = \frac{\text{particle surface}}{\text{particle volume}} \quad (36)$$

Rose and Wyllie To determine permeability from irreducible water saturation and formation resistivity factor, they

suggested modifying the Carman-Kozeny equation. They make a lot of assumptions regarding their equation. First, there is no difference between minimal and irreducible water saturation. Second, the grain surface's linear relationship to this water saturation number makes sense. Lastly, the electrical conductivity and fluid flow of the wetting phase is both impacted by the porous media's tortuosity [46].

$$K = \frac{P\phi^Q}{S_{wi}R} \tag{37}$$

Where, the Wyllie-Rose connection is a generalized equation that needs the values of the variables P, Q, and R to be calibrated based on primary measurements.

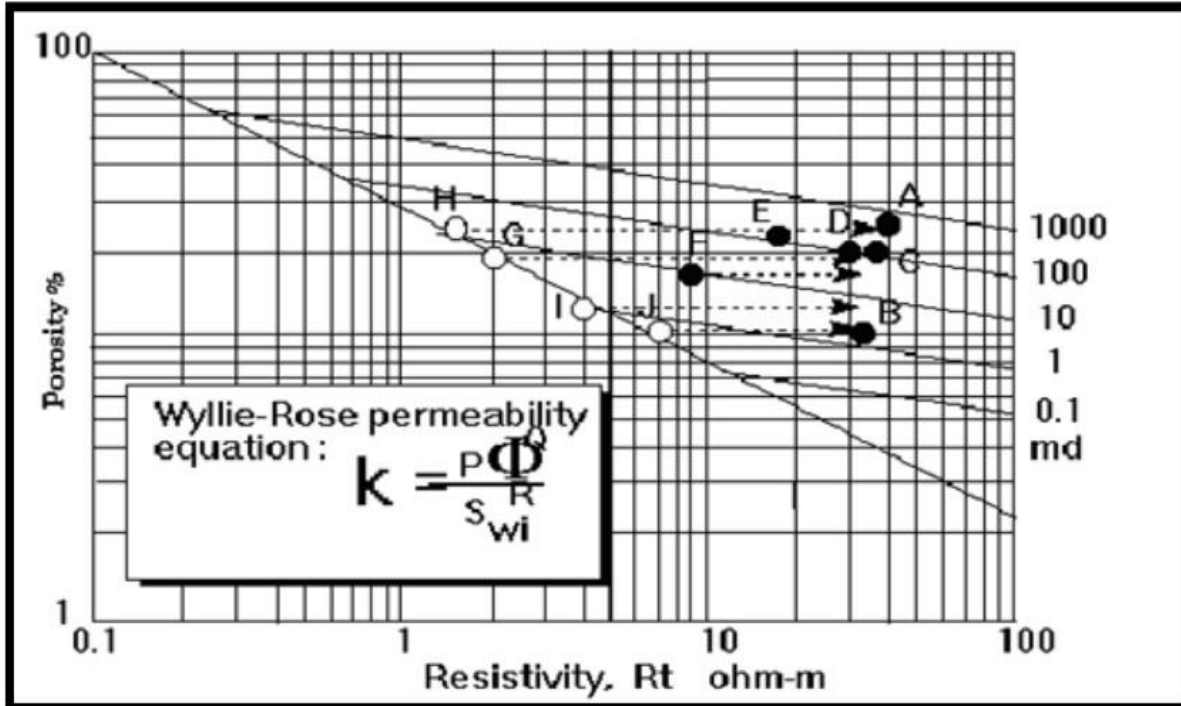


Figure 4: Permeability contours drawn on Pickett plot of Sandstone data, using a Wyllie-Rose relationship with both porosity and irreducible water saturation [47].

Tixier, the Wyllie Rose equation was used by the Tixier equation to produce the experimental permeability equation. The results of the Tixier equation roughly matched the results of the Morris-Biggs gas equation's permeability calculations[48].

Gary and Fatt We looked into how stress affected sandstone permeability and discovered that not only did rock permeability depend on overburden pressure, but that many sandstones also exhibit permeability anisotropy and that the ratio of radial to axial stress also affected how much permeability was reduced as a result of stress[49].
 Morris Biggs. Based on the Wyllie Rose equation, we offered permeability equations for oil and gas reservoirs. Timur's permeability calculation and Morris-Biggs' permeability in an area completely gas saturated (at irreducible water saturation) differ slightly. Unlike the Timur model, which depends on the effective porosity of gas reservoirs and irreducible water saturation, the permeability equation for gas fields is presented[50].

$$K^{1/2} = C \frac{\phi^3}{S_{wi}} \tag{38}$$

Where, C = constant, oil =250, gas =80.

Asnul Bahar (1997) proposes a method for producing reliable lithofacies distributions and ongoing petrophysical characteristics. The approach is a conditional simulation method that respects the data's top-notch distribution and the corresponding spatial connection. The technique successfully generated information about the types, distributions, and permeabilities of rocks in the sandstone and carbonate fields [52].

Timur suggested an equation to calculate permeability utilizing in-situ observations of remaining water saturation and formation porosity. He evaluated various hypotheses in the lab using 155 samples of sandstone from three oil fields to measure permeability, porosity, and residual water saturation. The main constraint of this equation is the constant value of the cementation exponent (m), which is equal to 1.5, while this variable may have other values in specific conditions[51].

Winland Applying the Winland hydraulic flow unit approach to the core data, five groups were created to predict permeability based on pore throat size at a 35% mercury saturation. Permeability and porosity measurements on core samples may be used to compute the r35 parameter, combined with additional petrophysical, geological, and engineering information to identify flow units in five carbonate reservoirs [53].

$$\log r_{35} = 0.732 + 0.588 \log k - 0.8641 \log \phi \tag{39}$$

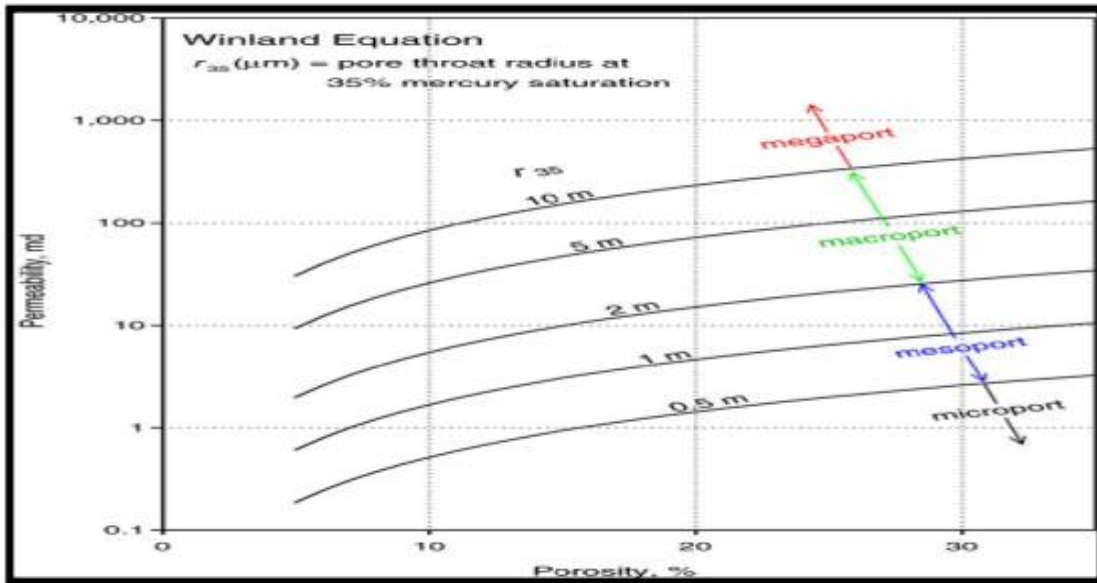


Figure 5: Empirical model based on regression attributed to Winland [53].

Figure (5), Be aware that permeability rises roughly in proportion to the square of the pore throat radius at a fixed porosity. The relationship between permeability and porosity for a given neck size is somewhat less than 2.

Additionally, Hartmann and Coalson claim that r₃₅ is a reliable indicator of the biggest connected pore throats in rock with intergranular porosity depends on entry size and pore throat sorting [54].

Coates and Dumanoir, the connection of permeability estimations of average gravity oil reservoirs, was presented [55],[56] based on irreducible water saturation and several forms of effective porosity.

$$K^{1/2} = \frac{C}{W^4} \frac{\phi^{2W}}{\frac{R_w}{R_{ti}}} \tag{40}$$

Where:

$$C = 23 + 465\rho h - 188\rho h^2 \quad \& \quad 2 = (3.75 - \phi) + \frac{1}{2} (\log_{10} (\frac{R_w}{R_{ti}}) + 2.2)^2 \tag{41}$$

Bo Shen et al. They developed a technique employing well logs to evaluate permeability in gluten reservoirs. This method is based on the equivalent geometry parameter, the flow porosity, and the K-C model. The authors also provide a method for calculating flowing porosity that may be used by scientists interested in the flow of electrical current through pores. This technique yields a constant and precise answer for glutenite reservoirs with significant variability, although more challenging than the standard permeability estimation method[57].

3. Conclusion

The primary goal of this paper is to present a comprehensive overview of the evolution of the field of formative assessment, as well as the research and applications that are accessible to tackle the problem. Following a thorough study of several research and articles on formation evaluation investigations, the following conclusions were reached:

1. The gamma-ray (single clay indicator technique) to calculate shale volume is the most popular and accurate method for calculating shale volume. This procedure can be used for any shaly layer generation. The influencing element in estimating clay volume is The hole size, which relates to the amount of drilling mud in the hole, affects the gamma-ray record, and environmental changes can alter the reading.

2. Water saturation based on the resistivity concept has been proven with a clear description of Archie's constant, the many factors that affect SW in this equation, and the updated models in the shaly formation.

Water saturation based on Archie's equation is subject to uncertainty; it is unusual to set Archie's parameters (m, n, and a) independent of wettability, formation water salinity, porosity, and permeability; all of these factors contribute to Archie's equation being inaccurate due to heterogeneities where the Archie's equation is used in the clean formation.

3. The Pickett plot method is useful for assessing log segments quickly in wells with little petrophysics data.

4. Modified porosity values and UCS values are useful in various configurations. Modifications are only used in limestone and shale formations, but gamma-ray data make such alterations applicable in many rock formations. Because Sw is so important in reservoir evaluation, it should be evaluated using a variety of approaches and compared to core laboratory data to arrive at an appropriate number.

5. Since the rock parameters such as porosity, permeability, and lithology vary vertically or horizontally in the heterogeneous formation, it is predicted that m values would change according to these variations to produce accurate findings.

6. Unfortunately, two processes have an impact on the fluid content of the core:

- the flooding of mud and mud filtrate into adjoining formations.
- the release of confining pressure when the core is removed.

7. There are two sorts of permeability approaches: non-experimental and experimental. Some theoretical methods are used in non-experimental methods to approximate the permeability, considering a fully saturated domain (Kozeny Carman). In contrast, laboratory methods combine three types of classifications: capillary effects (saturated and unsaturated), flow regime (constant pressure and constant flow), and flow direction (unidirectional and radial); then, the mathematical model of the method is established, taking such a combination into account.

NOMENCLATURE

(CEC) Cation Exchange Capacity

(Φ_t) Total Porosity

(ρ_g) Average Particle Density of Rock

(ρ_f) Effective Fluid Density in Flushed (Invaded) Zone

(ρ_{mf}) A Density of Mud Filtrate

(ρ_{ma}) A Density of Matrix

(SEM) Scanning Electron Microscopes

(H.I.) Hydrogen Index

(UCS) Unconfined Compressive Strength

(ROP) Rate Of Penetration

(BVW) Bulk Volume Water

(MDT) Modular Dynamics Tester

(RQI) Reservoir Quality Index

(HFU) Hydraulic Flow Unit

(N) Water saturation exponent

(M) Cementation factor

(r35) The Pore Throat Radius At 35% Mercury Saturation

- (K) Air Permeability
 (Φ) Porosity In Percent Unit

Conflict of Interest: The authors declare no conflict of interest.

References

- [1] S. S. Zughar, A. A. Ramadhan, and A. K. Jaber, "Petrophysical Properties of an Iraqi Carbonate Reservoir Using Well Log Evaluation," *Iraqi J. Chem. Pet. Eng.*, vol. 21, no. 1, pp. 53–59, 2020.
- [2] R. M. Idan, A. L. M. Salih, O. N. A. Al-Khazraji, and M. H. Khudhair, "Depositional environments, facies distribution, and porosity analysis of Yamama Formation in majnoon oilfield. Sequence stratigraphic approach," *Iraqi Geol. J.*, pp. 38–52, 2020.
- [3] H. Liu, *Principles and applications of well logging*. Springer, 2017.
- [4] N. M. S. Numan, "A plate tectonic scenario for the Phanerozoic succession in Iraq," *Iraqi Geol. J.*, vol. 30, no. 2, pp. 85–110, 1997. [5] Y. Yu and H. Menouar, "An experimental method to measure the porosity from cuttings: Evaluation and error analysis," 2015.
- [6] M. Amiri, J. Ghiassi-Freez, B. Golkar, and A. Hatampour, "Improving water saturation estimation in a tight shaly sandstone reservoir using artificial neural network optimized by imperialist competitive algorithm—A case study," *J. Pet. Sci. Eng.*, vol. 127, pp. 347–358, 2015.
- [7] U. Ahmed, S. F. Crary, and G. R. Coates, "Permeability estimation: the various sources and their interrelationships," *J. Pet. Technol.*, vol. 43, no. 05, pp. 578–587, 1991.
- [8] N. A. S. al Al-Azazi, A. Alsrory, and M. Albaroot, "Effect evaluation of shale types on hydrocarbon potential using well logs and cross plot approach, Halewah oilfield, Sab'atayn Basin, Yemen," *Energy Geoscience*, vol. 3, no. 2, pp. 202–210, 2022.
- [9] J. Sam-Marcus, E. Enaworu, O. J. Rotimi, and I. Seteyeobot, "A proposed solution to the determination of water saturation: using a modelled equation," *J. Pet. Explor. Prod. Technol.*, vol. 8, no. 4, pp. 1009–1015, 2018.
- [10] Adeoti, L., Ayolabi, E.A. and James, P.L. (2009) 'An integrated approach to volume of shale analysis: Niger Delta example, Offrire Field', *World Applied Sciences Journal*, 7(4), pp. 448–452.
- [11] Kamel, M.H., Mohamed, M.M., 2006. Effective porosity determination in clean/shaly formations from acoustic logs. *Journal of Petroleum Science and Engineering*, 51 (3-4): 267-274
- [12] Mabrouk, W.M., Soliman, K.S. and Anas, S.S. (2013) 'New method to calculate the formation water resistivity (Rw)', *Journal of Petroleum science and Engineering*, 104, pp. 49–52.
- [13] J. M. Wheatley, N. S. Rosenfield, G. Heller, D. Feldstein, and M. P. LaQuaglia, "Validation of a technique of computer-aided tumor volume determination," *J. Surg. Res.*, vol. 59, no. 6, pp. 621–626, 1995.
- [14] A. F. Atanda and A. K. Mahmood, "Theoretical Framework for Multi-Agent Collaborative Knowledge Sharing for Competitiveness of Institutions of Higher...".
- [15] Serra O. *Fundamentals of well-log interpretation*. USA: Elsevier Science Publishing Company Inc; 1984.
- [16] Clavier C, Hoyle W, Meunier D (1971) Quantitative interpretation of thermal neutron decay time logs: part I. Fundamentals and techniques. *J Petrol Technol* 23(6):743–755. <https://doi.org/10.2118/2658-A-PA>
- [17] Bassiouni Z (1994) Theory, measurement, and interpretation of well logs. Henry L Doherty Memorial Fund of AIME, Society of Petroleum Engineers, Texas
- [18] Hughes, B., 1992. *Advanced Wireline and MWD Procedures*. Houston, TX 77032, USA.
- [19] Archie, G.E., 1942. *The Electrical Resistivity Log as an Aid in Determining Some Reservoir Characteristics*. Texas.
- [20] D.J. Hartmann, E.A. Beaumont Prediction reservoir systems quality and performance in exploring oil and gas traps AAPG Special Publication (1992)
- [21] Tixier, M.P., 1958. Porosity Balance Verifies Water Saturation Determined from Logs. *Journal of Petroleum Technology* 10, 161–169.
- [22] Schlumberger, n.d. *Log Interpretation Charts, D-12*. [29] Pickett, R.G., 1966. A Review of Current Techniques for Determination Of Water Saturation From Logs.
- [23] Pickett, R.G., 1966. A Review of Current Techniques for Determination Of Water Saturation From Logs.
- [24] Pickett, G.R., 1973. *Pattern Recognition As A Means Of Formation Evaluation*. The Log Analyst 14.
- [25] J. R. Fanchi, *Principles of applied reservoir simulation*. Elsevier, 2005.

- [26] S. Tandon, C. Newgord, and Z. Heidari, "Wettability quantification in mixed-wet rocks using a new NMR-based method," *SPE Reserv. Eval. Eng.*, vol. 23, no. 03, 24 pp. 896–916, 2020.
- [27] W. H. Nugent, G. R. Coates, and R. P. Peebler, "A new approach to carbonate analysis," 1978.
- [28] I. Odizuru-Abangwu, A. Suleiman, and C. Nwosu, "The impact of different shaly sand models on in place volumes and reservoir producibility in niger delta reservoirs-the dual water and normalized Waxman-Smiths saturation models," 2010.
- [29] Krygowski, D.A., Cluff, R.M., 2015. Pattern recognition in a digital age: a gameboard approach to determining petrophysical parameters. In: SPWLA 56th Annual Logging Symposium. OnePetro.
- [30] Leveaux, J., Poupon, A., 1971. Evaluation Of Water Saturation In Shaly Formations. *The Log Analyst* 12.
- [31] Poupon, A., Loy, M.E., Tixier, M.P., 1954. A Contribution to Electrical Log Interpretation in Shaly Sands. *Journal of Petroleum Technology* 6, 27–34.
- [32] Simandoux, P., 1963. Mesures dielectriques en milieu poreux, application a mesure des saturations en eau, Etude du Comportement des massifs Argileux. *Revue de l'Institut Français du Pétrole*, n Hors-Série 193–215.
- [30] Asquith, G.B., Krygowski, D., Gibson, C.R., 2004. Basic well log analysis. American Association of Petroleum Geologists Tulsa
- [31] Tittman, J., Wahl, J.S., 1965. The physical foundations of formation density logging (gamma-gamma). *Geophysics* 30, 284–294. [34] Wyllie, M.R.J., Gregory, A.R., Gardner, G.H.F., 1958. An experimental investigation of factors affecting elastic wave velocities in porous media. *Geophysics* 23, 459–493.
- [32] C. Barros and A. Andrade, "Determination of water saturation by intelligent algorithm," III SimBGf, 2008.
- [33] Waxman, M.H., Thomas, E.C., 1974. Electrical Conductivities in Shaly Sands-I. The Relation Between Hydrocarbon Saturation and Resistivity Index; II. The Temperature Coefficient of Electrical Conductivity. *Journal of Petroleum Technology* 26, 213–225.
- [34] Smits, L.J.M., 1968. SP log interpretation in shaly sands. *Society of Petroleum Engineers Journal* 8, 123–136.
- [35] E. C. Onyia, "Relationships between formation strength, drilling strength, and electric log properties," 1988.
- [36] V. Matko, "Porosity determination by using stochastics method," *Autom. časopis za Autom. Mjer. Elektron. računarstvo i Komun.*, vol. 44, no. 3–4, pp. 155–162, 2003.
- [37] B. Erfourth, C. Wright, N. Hudyma, and M. MacLaughlin, "Numerical Models of Macroporous Rock: Quantifying the Influence of Void Characteristics on Elastic Modulus," *Golden Rocks 2006, The 41st U.S. Symposium on Rock Mechanics (USRMS)*. p. ARMA-06-963, Jun. 17, 2006.
- [38] M. A. Westbrook and J. F. Redmond, "A new technique for determining the porosity of drill cuttings," vol. 165, no. 01, pp. 219–222, 1946.
- [39] P. Horsrud, "Estimating mechanical properties of shale from empirical correlations," *SPE Drill. Complet.*, vol. 16, no. 02, pp. 68–73, 2001.
- [40] S. Siddiqui, A. S. Grader, M. Touati, A. M. Loermans, and J. J. Funk, "Techniques for extracting reliable density and porosity data from cuttings," 2005.
- [41] R. Lenormand and O. Fonta, "Advances in measuring porosity and permeability from drill cuttings," 2007.
- [42] Hamada, G.M. (1996) 'An integrated approach to determine shale volume and hydrocarbon potential in shaly sand', in SCA International Symposium, pp. 2093–2107.
- [43] V. Matko, "Porosity determination by using stochastics method," *Autom. časopis za Autom. Mjer. Elektron. računarstvo i Komun.*, vol. 44, no. 3–4, pp. 155–162, 2003.
- [44] D. J. Hartmann, E. A. Beaumont, and N. H. Foster, "Predicting reservoir system quality and performance," *Explor. oil gas traps AAPG Treatise Pet. Geol. Handb. Pet. Geol.*, pp. 1–9, 1999.
- [45] Y. Kuang, L. Sima, Z. Zhang, Z. Wang, and M. Chen, "A model for estimating the saturation exponent based on NMR in tight sandy conglomerate reservoirs," *Arab. J. Sci. Eng.*, vol. 43, no. 11, pp. 6305–6313, 2018.
- [46] M. Wyllie, "Evaluation of permeability from electric-log resistivity gradients," *Oil Gas J.*, vol. 16, pp. 113–133, 1949.
- [47] W. L. Watney, J. H. Doveton, and W. J. Guy, Development and demonstration of an enhanced spreadsheet-based well log analysis software. Final report, May 1998," Kansas Geological Survey, Lawrence, KS (United States), 1998.25
- [48] N. E. Stauff, K. Biegel, W. N. Mann, and B. Dixon, "Feb. 2021 Electricity Blackouts and Natural Gas Shortages in Texas," Argonne National Lab.(ANL), Argonne, IL (United States), 2021.

- [49] D. H. Gray and I. Fatt, "The effect of stress on permeability of sandstone cores," *Soc. Pet. Eng. J.*, vol. 3, no. 02, pp. 95–100, 1963.
- [50] M. Abdideh, N. B. Birgani, and H. Amanipoor, "Estimating the reservoir permeability and fracture density using petrophysical logs in Marun oil field (SW Iran)," *Pet. Sci. Technol.*, vol. 31, no. 10, pp. 1048–1056, 2013.
- [51] S. Cannon, *Petrophysics: a practical guide*. John Wiley & Sons, 2015.
- [52] M. El-Bagoury, "Integrated petrophysical study to validate water saturation from well logs in Bahariya Shaley Sand Reservoirs, case study from Abu Gharadig Basin, Egypt," *J. Pet. Explor. Prod. Technol.*, vol. 10, no. 8, pp. 3139–3155, 2020.
- [53] D. V. Ellis and J. M. Singer, *Well logging for earth scientists*, vol. 692. Springer, 2007.
- [54] S. Deng, Q. Sun, H. Li, N. Huo, and X. He, "The sensitivity of the array resistivity log to mud filtrate invasion and its primary five-parameter inversion for improved oil water recognition," *Pet. Sci.*, vol. 9, no. 3, pp. 295–302, 2012.
- [55] R. F. Aguilera, "A triple porosity model for petrophysical analysis of naturally fractured reservoirs," *Petrophysics-The SPWLA J. Form. Eval. Reserv. Descr.*, vol. 45, no. 02, 2004.
- [56] K. Yazdchi, S. Srivastava, and S. Luding, "On the validity of the Carman-Kozeny equation in random fibrous media," in *PARTICLES II: proceedings of the II International Conference on Particle-Based Methods: fundamentals and applications*, 2011, pp. 264–273.
- [57] C. Haro, "The theory behind the Carman–Kozeny equation in the quest for permeability of the Rocks," *GeoConvention Integr.* 5th–10th May, Calgary, Canada, 2013.
- [58] Darling, T., 2005. *Well logging and formation evaluation*. Elsevier.